How to cite: *Angew. Chem. Int. Ed.* **2022,** *61,* e202212112
International Edition: doi.org/10.1002/anie.202212112
German Edition: doi.org/10.1002/ange.202212112

Cage Compounds

Steering the Ultrafast Opening and Closure Dynamics of a Photochromic Coordination Cage by Guest Molecules

*Kevin Artmann, Ru-Jin Li, Selina Juber, Elie Benchimol, Lars V. Schäfer, Guido H. Clever, and Patrick Nuernberger**

Abstract: Photochemical studies on supramolecular hosts that can encapsulate small guest molecules commonly focus on three aspects: photoswitching the cage to release or trap the guest, the effect of the confining environment on the guest, and light-induced exciton or charge transfer within the cage structure. Here, we exploit ultrafast spectroscopy to address how the guest alters the photoswitching characteristics of the cage. For this, the impacts of three disparate guest compounds on ring-opening or ring-closure of a dithienylethene (DTE) ligand in a photoswitchable DTE-based coordination cage are juxtaposed. The guest modulates both outcome and timescale of the cage's photodynamics, by an interplay of structural strain, heavy-atom effect, and enhancement of charge-transfer processes exercised by the guest on the photo-excited cage. The approach might prove beneficial for attuning the applicability of photoswitchable nanocontainers and desired guest compounds.

Introduction

The confinement of molecules by pores, nanocontainers, micelles, or macromolecular structures has a multitude of applications, ranging from controlled transport and delivery of guest compounds to optimized environments for catalytic reactions inside the nanocage. As one of many versatile directions, the use of organic frameworks or self-assembled coordination cages for this purpose has been advanced over the last decades,[1–11] with light-induced exciton or charge-transfer dynamics opening up new routes for synthesis involving host–guest systems.[12–15] A further functionality can be added if the cage can be switched by an external stimulus, for instance by light, allowing the controlled uptake or release of such guest molecules.[16–21] Furthermore, when host–guest systems are illuminated, the interactions of the host with the guest may change the photodynamics of the latter, as has been monitored with time-resolved spectroscopy for molecules in cyclodextrins,[22–24] silica-based materials,[25] metal–organic frameworks,[26,27] or self-assembled nanocages.[13,28,29]

In contrast to this behavior aiming at modification of the guest, host–guest interactions may just as well affect the dynamics following excitation of a photochromic host. In this Article, we will pursue this approach by ultrafast spectroscopy studies on a supramolecular cage that can undergo reversible guest encapsulation.[30–32] It comprises four DTE molecules (Figure 1a, top) that coordinate to two Pd^{II} cations in a square-planar orientation, yielding a cavity defined by the banana-shaped DTE ligands (Figure 1a, bottom).

As shown in Figure 1a, the DTE ligand can be reversibly switched between a colorless open (L_O) and a blue-colored closed isomer (L_C). Upon UV excitation of L_O, a conrotatory ring-closure reaction leads to an elongated π-delocalization. Therefore, the π-π* excitation is strongly red-shifted, giving rise to the intense color of L_C. X-ray structures could identify supramolecular cages with all ligands open (C_{4O}), with two open and two closed ligands (C_{2O2C}) and with four closed ones (C_{4C}),[33] indicating that the interconversion from the all-open C_{4O} to the all-closed C_{4C} isomer of the cage is a stepwise process that proceeds via intermediates.

Similar to other DTE systems,[34–37] the open form L_O can exist in multiple stable conformers that can interconvert at room temperature. Typically, DTEs possess an antiparallel (AP) and a parallel (P) form where the two side groups point in opposite directions or in the same direction, respectively. However, the conrotatory ring-closure reaction can only occur from the AP conformation.[34,35,38] Hence, the quantum yield for cyclization can be enhanced by increasing the ratio of the AP conformer, e.g. by introducing bulky substituents[39] or intramolecular noncovalent interactions.[40] In the supramolecular cage C_{4O}, the open DTE ligands are already trapped in a conformation similar to the AP form,

[*] K. Artmann, Prof. Dr. P. Nuernberger
Institut für Physikalische und Theoretische Chemie, Universität Regensburg
93040 Regensburg (Germany)
E-mail: patrick.nuernberger@ur.de
Homepage: https://go.ur.de/photochem
Dr. R.-J. Li, E. Benchimol, Prof. Dr. G. H. Clever
Department of Chemistry and Chemical Biology, TU Dortmund University
44227 Dortmund (Germany)
S. Juber, Prof. Dr. L. V. Schäfer
Theoretical Chemistry, Ruhr University Bochum
44780 Bochum (Germany)

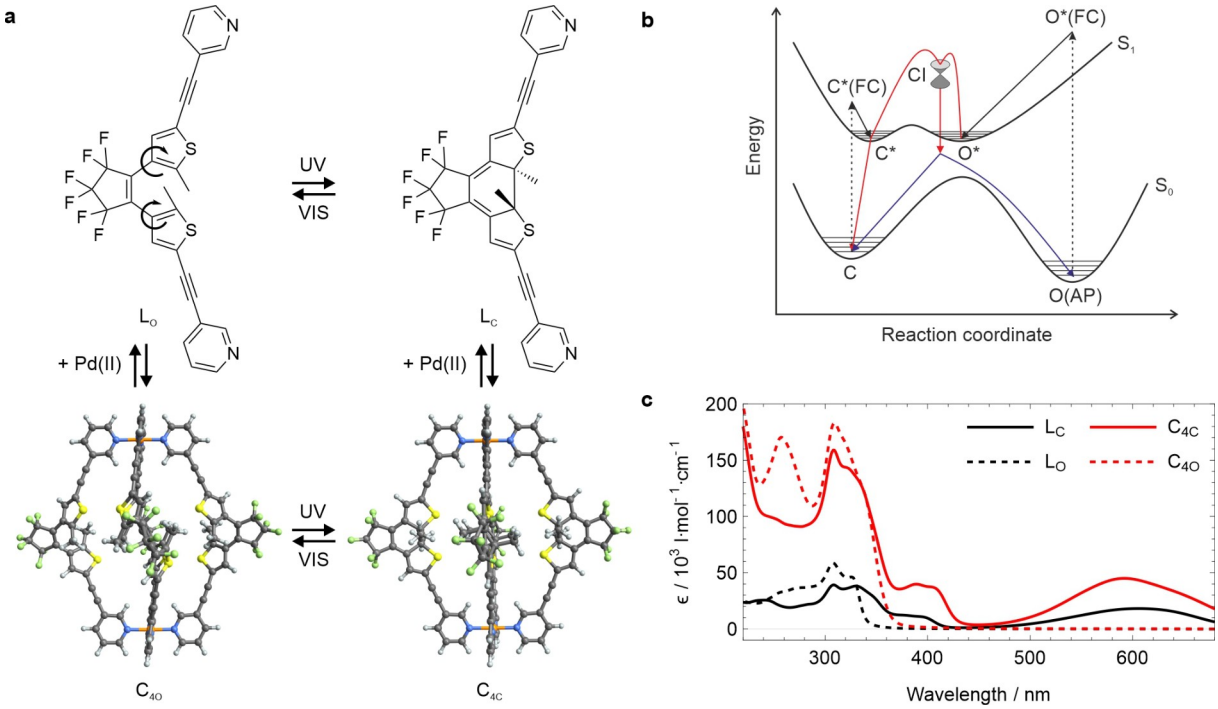

Figure 1. a) Reversible photoswitching of the DTE-based ligand (top), four of which form the supramolecular cage (bottom). b) Sketch of the PESs of dithienylethene (DTE) illustrating the photochromism (adapted from ref. [35]). c) Absorption of the four species shown in panel (a).

allowing photocyclization. In L_C, the additional carbon-carbon bond prevents a reorientation of the thiophene side groups, yielding only one stable closed conformer both for free DTE molecules and for DTE ligands in the cage.

The underlying processes that describe the photochromism of DTE systems have been investigated extensively by experimental and computational approaches. It is generally assumed that only singlet states are relevant for their photochromism. However, experimental evidence for a photocyclization including triplet states was found by De Cola and co-workers[41,42] who showed that a DTE ligand that acts as a bridge between two $Ru(bpy)_3$ units undergoes an oxygen sensitive ring-closure on a nanosecond time scale. Furthermore, laser flash photolysis studies[43] unveiled that cyclization from the triplet state on a microsecond timescale is also possible for metal-free systems. This was confirmed by Aloïse and co-workers[44,45] who found that by constraining the molecule's geometry with a bridge, the triplet state is populated and participates in the cyclization reaction occurring on a microsecond timescale. As the primary steps of the photodynamics of DTE systems occur on a picosecond timescale, it is generally accepted that conical intersections (CIs) are involved in the ultrafast dynamics. Complete Active Space Self Consistent Field (CASSCF) quantum chemical calculations revealed that ring-opening and closure both share the same CI that is dynamically accessible from the closed and the open conformer.[46] It was also disclosed that the CI is not on the direct reaction path (confer Figure 1b) and therefore a relaxation on the potential energy surface (PES) of the excited state S_1 precedes the transition through the CI. Furthermore, an energy barrier on the S_1 PES, being closer to the geometry of the closed conformer, was reported in several theoretical studies,[46,47] and experiments corroborate such an S_1 energy barrier because the efficiency of the ring-opening rises with higher excitation energy[48] and also with higher temperature.[49] Ultrafast studies by the groups of Kryschi,[50–54] Irie,[35,55–57] and Miller[58–60] are in good accordance with the theoretical predictions and show that the dynamics of the cyclization can be separated into three different stages: The pre-switching, ring-closure and post-switching.[35] The pre-switching describes the motion on the S_1 PES from the Franck–Condon region O*(FC) to the relaxed geometry O*, occurring on the sub-ps timescale and detectable by a spectral blue-shift of the excited-state absorption (ESA) within 1 ps.[58] The ring-closure depicts the transition through the CI that leads to a branching to the ground state of open and closed conformers. The decay constants associated with ring-closure depend on the DTE system under study, but in general this process takes less than 10 ps. It is followed by the post-switching that incorporates vibrational cooling in the ground state. The investigation of the cycloreversion (ring-opening) is experimentally more challenging as there is no distinct absorption of the open form in the visible spectral region. However, Irie, Miyasaka and co-workers[57] investigated the temperature dependence of the cycloreversion and concluded from comparison with theoretical studies that there is a rapid deactivation from the relaxed geometry of the S_1 state (C*→C) competing with an activated pathway through the CI that leads to the photoproduct (C*→CI→C/O). By increasing the temperature, the latter path is enhanced.

In this work, three anionic guest molecules are employed that differ in their shape and electronic properties but that can all bind inside the DTE-based cage. Figure 2 shows the structures and electrostatic potentials as obtained by density-functional theory (DFT) calculations. The $[B_{12}F_{12}]^{2-}$ anion (G1) has a spherical shape with the negative charge distributed homogeneously over the whole surface, as is imposed by the icosahedral symmetry. In contrast, in the benzene-1,4-disulfonate (G2) and 1,1′-bis(sulfonato)ferrocene (G3) anions, the negative charge is localized at the sulfonate groups. Although entropic contributions play a crucial role for the overall thermodynamics of guest encapsulation,[30,33,61] the different electrostatic interactions with the cage may impact the dynamics of the surrounding structure. Furthermore, as the influence of triplet states was already shown for the cyclization reaction,[41–44] the ferrocene guest and the Pd^{II} ions might, to a certain degree, promote intersystem crossing (ISC) via the heavy-atom effect.[62] In the coordination cage, a further photoinduced effect, which is not possible in the free ligand, may contribute in the form of a charge transfer process involving the excited ligand and a palladium atom.[63,64]

For the $[B_{12}F_{12}]^{2-}$ dianion, NMR titration and isothermal titration calorimetry (ITC) previously disclosed that it binds to both the open (C_{4O}) and the closed (C_{4C}) cage, yet the affinity to C_{4O} ($K_a = 3.2\times10^4\ M^{-1}$) is higher than to C_{4C} ($K_a = 6.7\times10^2\ M^{-1}$).[30,33] These experiments substantiated that the guest encapsulation is entropy driven and favored for the open cage, with solvation and structural flexibility of the cage (which is highest for C_{4O}) presumably playing major roles in controlling the guest affinity. Encapsulation of a chiral guest in the open cage further revealed that the chiral information can be transferred between the guest and the host.[65] However, those experiments also indicated that the closure of the first ligand already leads to the ejection of the guest molecule. We recently investigated the encapsulation of $[B_{12}F_{12}]^{2-}$ by MD simulations and found that the entropic driving forces of the guest encapsulation process are related to solvation, as the guest molecule has to partially strip off its ordered solvation shell upon binding inside the cavity of the cage.[61] Stepwise light-induced ring-closure of the DTE ligands leads to a gradual decrease of the binding affinity of the guest, with the largest loss of affinity caused by closing the first DTE ligand,[61] further supporting the notion that the guest unbinds from the cage already after photoinduced closure of the first ligand. Here, we focus on the ultrafast dynamics of the supramolecular cage and investigate how these dynamics change upon encapsulation of different guest molecules which themselves are not excited.

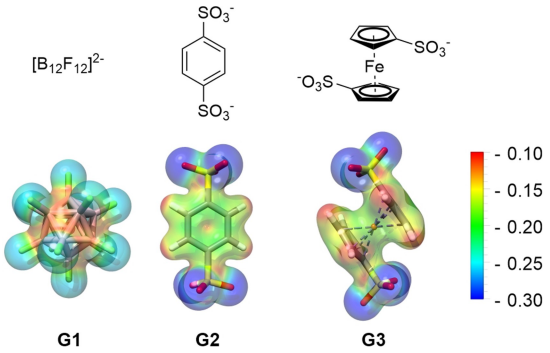

Figure 2. Guest anions and their electrostatic potentials (au), mapped onto the 0.02 au isosurfaces of the electron density.

Results and Discussion

Quantum Chemical Calculations

In C_{4O}, the ligand is trapped in a conformation close to the AP form, whereas there are multiple configurations possible for the free open ligand L_O. In order to identify those structures, a two-dimensional relaxed potential energy scan was conducted, where both thienyl groups were rotated. The exact procedure is described in the Supporting Information. Hereby, four different conformers were identified: the antiparallel conformer L_O(AP) and three additional conformers where one ($L_O(P_{1,2})$) or both ($L_O(P_3)$) thienyl substituents are rotated (see Table S2 in Supporting Information). For all obtained structures a geometry optimization was performed at the B3LYP-d4/TZVP level of theory, with solvation in acetonitrile included using the continuum solvation model COSMO.[66] The relative energies $\Delta E = E - E(AP)$ for all conformers are shown in Table 1. Indeed, the antiparallel conformation L_O(AP) is the lowest energy structure and therefore the predominant species, allowing for a direct comparison between the transient data of the free ligand and the cage. However, due to the relatively small energy differences obtained for the parallel conformers, we expect a non-negligible contribution of the parallel form on the experimental data of the free ligand.

The structures of the cages occupied by a guest molecule were optimized in implicit acetonitrile solvent at the B3LYP/6-31G* level of theory. Table S3 in the Supporting Information contains key structural parameters of the fully closed and fully open cages, which were also studied in the transient absorption (TA) measurements, together with distances and dihedral angles that possibly affect the ultrafast photodynamics. Table 2 summarizes the characteristic distances and dihedral angles of the cage before and after encapsulation of the guest molecules, where each value was averaged over all four photochromic DTE units. In case of

Table 1: Relative energies and the dihedral angles α_1 and α_2 that describe the rotation of the two thienyl groups for all conformers of the DTE ligand.

	ΔE [kJ mol^{-1}]	α_1	α_2
L_O(AP)	0.0	133.0	135.9
$L_O(P_1)$	5.4	129.9	−36.7
$L_O(P_2)$	8.0	−48.8	132.8
$L_O(P_3)$	14.8	36.2	58.5
L_C	61.5	174.0	173.8

All calculations were conducted at the B3LYP-d4/def2-TZVP level of theory and solvation was considered using the continuum solvation model COSMO.[66]

Table 2: Characteristic distances [in Å] and dihedral angles [in degrees] of the cages, averaged over the four photochromic units.[a]

Cage	Guest	d_{CC}[b]	α_{MeCCMe}[c]	α_{CCCC}[d]
C_{4C}	none	1.55	175.5	10.2
	G1	1.55	174.3	10.0
	G2	1.55	176.3	10.3
	G3	1.55	176.4	10.4
C_{4O}	none	3.69	167.9	7.7
	G1	3.71	160.2	7.7
	G2	3.75	177.6	6.3
	G3	3.71	172.7	7.4

All values were obtained at the B3LYP/6-31G* level of theory in implicit acetonitrile. A list of all structural parameters is given in Table S3. [a] averaged over the four photochromic units *i*, e.g. $d_{CC} = \frac{1}{4}\sum_{i=1}^{4}|d_{CC,i}|$. [b] distance between the C-atoms that form the bond upon ring-closure. [c] dihedral angles between the two methyl substituents (C_1-C_2-C_{10}-C_{11}). [d] dihedral angles between the two aryl groups (C_3-C_4-C_8-C_9).

the fully closed cage, these values are only slightly affected by the presence of the guest molecule. As a consequence, in the TA measurements, we do not expect to see a pronounced impact caused by steric strain of the encapsulated guest molecule. In contrast, the presence of the guest modifies the characteristic angles and distances of the open cage. Due to the flexibility of the open cage, the steric strain induced by the guest molecule leads to a deformation of the ligands in the cage, thereby possibly also affecting the ultrafast dynamics of the cage.

Cycloreversion (Ring-Opening)

For the investigation of the ring-opening dynamics with ultrafast TA spectroscopy, the closed forms of the free ligand L_C, of the empty cage C_{4C}, and of the cage encapsulating the different guest molecules ($G@C_{4C}$) were excited with femtosecond pulses centered at 600 nm. For all measurements, the sample reservoir was continuously irradiated with UV light to prevent an increase of the concentration of the open isomers. In the following, the data are interpreted by scrutinizing the transient spectra obtained on different time scales. All datasets were also dissected by global analysis (time constants and decay-associated difference spectra (DADS) given in the Supporting Information), from which also all the time constants discussed here originate.

The ring-opening dynamics of L_C are displayed in the left column of Figure 3. Initially, the TA signal is dominated by a broad ESA that overlaps with a ground-state bleach (GSB) above 550 nm and below 360 nm. There is no distinct blue-shift within 0.5 ps after excitation (black curves in Figure 3), as was also not observed in other studies on similar ring-closed DTE compounds.[54,57,58] This might originate from the low excess energy directly after excitation and the similarity between the excited closed isomer in the C*(FC) and C* geometry (Figure 1b), in contrast to the situation for L_O (vide infra). The further evolution of the

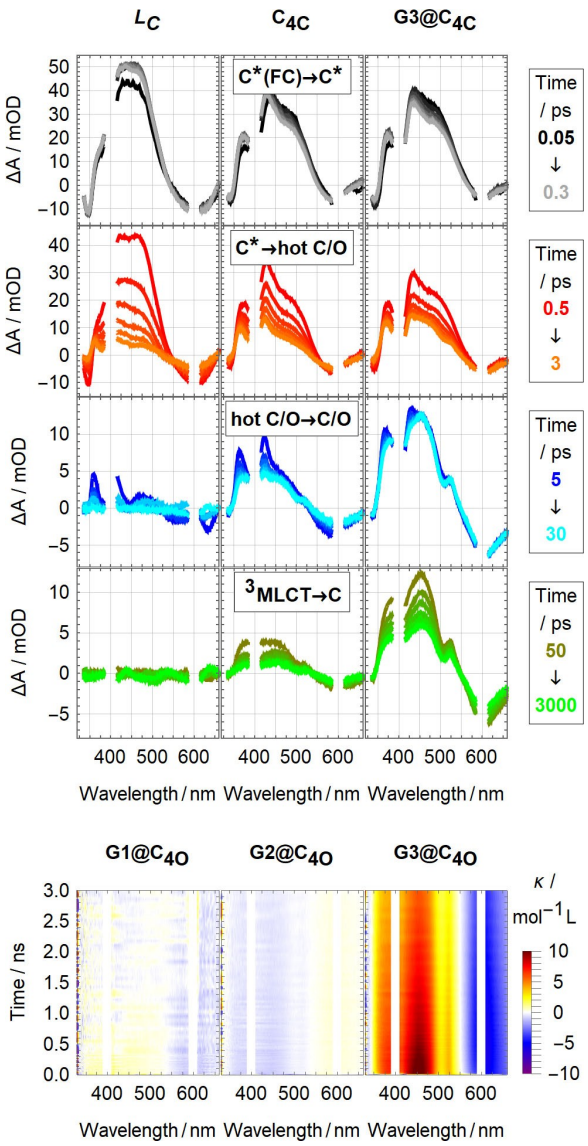

Figure 3. Ultrafast dynamics of the closed conformers upon excitation at 600 nm. Top: Δ*A* of a 4 mmol L^{-1} solution of the free ligand (left), Δ*A* of a 1 mmol L^{-1} solution of the cage (center), and Δ*A* of the cage after addition of one equivalent G3 (right). Bottom: Change of the transient signal $\kappa(t,\lambda)$ induced by the guest encapsulation.

TA signal can be described with two spectral components: First, a decay of the broad ESA with a lifetime of 1 ps (evident from the red curves) is accompanied by a recovery of the GSB above 550 nm. Taking the PES (Figure 1b) from the literature as a basis, this species can be assigned to the relaxed excited state C* from which either the ring-opening through the shared CI (C*→CI→hot C/O) or the direct transition to the ground state (GS) of the closed form (C*→hot C) can occur. Thus, the lifetime of 1 ps can be assigned to the ring-opening process. Second, a narrower positive signal around 400 nm decays with a lifetime of 5 ps. As depicted by the corresponding DADS (blue line in Figure S5c), this decay is also accompanied by a rising signal above 550 nm. As the minimum of the DADS is red-shifted

compared to the stationary absorption of the closed form, this is GSB recovery caused by vibrational cooling. Hence, this time constant can be assigned to the vibrational relaxation of the hot closed or open form after transition to the GS (hot C/O→C/O). Since no TA signals remain after 30 ps (see green spectra for L_C), we conclude that the quantum efficiency of ring-opening of this DTE is very small, as also reported for similar DTE systems.[35] Thus, most molecules that pass the CI will return to the ground state of the closed isomer.

The ring-opening dynamics of the cage C_{4C} are shown in the middle column of Figure 3. From a probability estimation, one can deduce that the most likely scenario is the one in which only one of the four DTE ligands is excited in a cage, and thus also just this one ligand may ring-open. The initial dynamics for C_{4C} are similar to those of L_C. The ring-opening also occurs with a time-constant of approximately 1 ps. However, the amplitude of this spectral component is significantly smaller than for L_C, which already indicates that reaching the S_1 minimum structure is less likely. Identical to the free ligand, the ring-opening is followed by vibrational cooling of the hot closed and open forms. The most remarkable difference however is the presence of an additional dynamic which was not present for L_C. As depicted by the green curves in Figure 3, an additional positive signal below 550 nm is observed which decays with a lifetime in the nanosecond regime ($\tau_3 > 1$ ns) and which is also accompanied by a GSB recovery. One might argue that the observation of GSB for a prolonged time might be indicative of an enhanced quantum yield for ring-opening, but we refrain from this interpretation because of the additional spectral component that is not characteristic for a ring-open ground-state DTE species, which usually only absorb in the UV. Furthermore, a transition from the S_1 state is unlikely, as the lifetime of the S_1 state is determined by the velocity of the transition through the CI. An ISC to the ligand-centered triplet state is unlikely, as it was already demonstrated that the triplet states of diarylethenes typically exhibit a lifetime in the microsecond regime.[43–45,67] However, Jukes et al. found for a diarylethene that acts as a bridge between two Ru or Os atoms, that a charge transfer between ligand and metal can occur. The ^{1}MLCT state converts into the ^{3}MLCT state by ISC, which subsequently decays within tens to hundreds of nanoseconds depending on the metal and ligand structure. They demonstrated that phosphorescence from the ^{3}MLCT occurs. We thus performed time-resolved emission experiments for the cage systems investigated here, and an analogous emission (described in detail in the Supporting Information) was observed, with a decay time being close to the time constant τ_3 found in ultrafast TA for the same systems. Hence, the dynamics characterized by τ_3, only present in the cage and associated with a competitive deactivation path to the relaxation from S_1, can be identified as relaxation of the ^{3}MLCT state. This should further reduce the small efficiency of the ring-opening reaction compared to the free ligand.

For all guest molecules, TA measurements were performed for five different host:guest stoichiometries, yielding 15 independent data sets with differing amounts of filled cages with four closed ligands (see Table S1 for all individual concentrations and all determined time constants, as well as NMR data in Figure S1 to S4 corroborating guest encapsulation). Exemplarily, the temporal development of the TA signal after addition of one equivalent of G3 is shown in the right column of Figure 3 ($G3@C_{4C}$). It can be seen that all three spectral components that are present for C_{4C} are also visible when G3 occupies the cavity of the cage. However, the slowest one that is assigned to the transition from the ^{3}MLCT state back to the ground state of the closed isomer is much more pronounced. By contrast, the contribution of both the deactivation from the S_1 state (red curves) and the subsequent vibrational cooling (blue curves) decrease significantly, which reveals that the encapsulation of G3 decreases the ring-opening efficiency by an increased population of the ^{3}MLCT state.

To visualize how large the impact of the guest on the photodynamics of the cage is, we have calculated the change $\kappa(t,\lambda)$ (see Supporting Information for a description) of the TA signal as caused by the presence of the guest. The results are shown in the bottom panels of Figure 3. Guests G1 and G2 have only little influence on the photodynamics setting in after exciting the bound cages $G1@C_{4C}$ or $G2@C_{4C}$, as can be derived from tiny $\kappa(t,\lambda)$ values indicating only slight changes. Therefore, we conclude that effects such as the steric strain present in the cage when the guest is bound[61] and electrostatic interaction between the anionic guest and the cationic cage do not impact the ring-opening dynamics. Interestingly, the case of $G3@C_{4C}$ is remarkably different, with large $\kappa(t,\lambda)$ values. We infer that the ferrocene guest further increases the population of the ^{3}MLCT state presumably through a heavy-atom effect.

These observations are in good accordance with the geometries that were obtained for the host–guest complex. If steric strain inside the cage or electrostatic interactions between the host and the guest would have a significant influence on the dynamics of the cage, this should be reflected in a corresponding distortion of the ligands in the cage. While the optimized geometries of the occupied closed cages look slightly deformed (see $G@C_{4C}$ structures in Table S3), the individual ligand's geometry is nearly identical to the empty cage (compare Table 2). Thus, the quantum-chemical calculations also support the assumption that another effect like an enhanced ISC or a charge transfer gives rise to the drastic change of the photodynamics after addition of the ferrocene guest.

Cyclization (Ring-Closure)

For studies on the ultrafast cyclization dynamics, excitation with pulses centered at 310 nm were employed. For all measurements, the sample reservoir was continuously irradiated with visible light to prevent an increase of the concentration of the closed isomers during the time course of the experiments. Again, all time constants were obtained by global analysis and are listed in the Supporting Information together with the DADS.

The dynamics of excitation of L_O are shown in Figure 4. Initially, a broad ESA that peaks at 490 nm covers the complete visible spectrum, and a spectral blue-shift on a femtosecond timescale (black curves) is observed, in contrast to the dynamics after excitation of L_C. This agrees well with previous observations by Miller and co-workers[58] who assigned the shift to relaxation on the S_1 PES (O*(FC)→O). The spectral shift includes a spectral broadening which was already observed for a different DTE derivative by Duppen and co-workers.[68,69] This blue-shift is followed by two processes whose lifetimes are nearly identical to those found in the cycloreversion: on the one hand, a decay of the broad ESA with a lifetime of 1.4 ps is accompanied by a rising product absorption (PA) at 600 nm (red curves); on the other hand, a decay of a narrower positive signal below 550 nm with a lifetime of 18 ps (blue curves) can be seen. Due to the temporal and spectral similarity, those spectral components are identified as the same two processes that were already observed for the cycloreversion. The short-lived component is assigned to the ring-closure reaction through the shared CI (O*→CI→hot O/C), whereas the longer time-constant describes the vibrational cooling after transition to the GS (hot O/C→O/C). In addition, the experimental spectra show a fourth dynamical component with a lifetime of about 100 ps (purple curves). Since this component is not present if the ligand is bound to the cage, these dynamics are assigned to the transition from the excited state of the parallel conformer (P) back to the ground state (O*(P)→O). After 300 ps, a constant signal similar to the spectrum of L_C (Figure 1c) remains, corroborating that ring-closure is completed on a ps time scale.

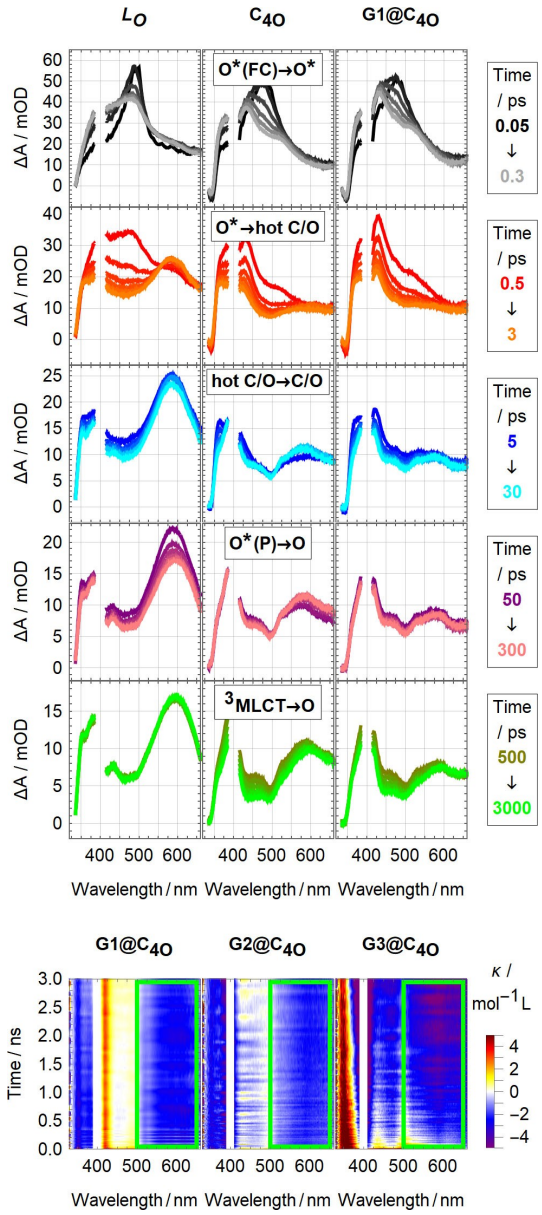

Figure 4. Ultrafast cyclization dynamics of the open isomers observed after excitation with 310 nm. Top: ΔA of a 4 mmol L^{-1} solution of the free ligand (left), ΔA of a 1 mmol L^{-1} solution of the cage (center), and ΔA of the cage after addition of five equivalents of G1 (right). Bottom: Change of the transient signal $\kappa(t,\lambda)$ induced by the guest encapsulation.

When exciting a cage C_{4O} with four open ligands, the spectral cuts in the middle column of Figure 4 show dynamics similar to the case of L_O. All spectral components that were observed for the antiparallel configuration of the free ligand, i.e. the relaxation in the excited state (black curves), the transition to the GS (red curves) and the vibrational relaxation within the GS (blue curves), are also visible for the cage with time constants of <1 ps, 1.5 ps and 15 ps, respectively. Two observations are most remarkable: first, the positive signal around 600 nm is smaller, indicating less ring-closure. In contrast to the cycloreversion, the transition from O* to the CI (red curves) does not show a pronounced rise of the PA at 600 nm. Thus, the ring-closure through the CI seems to be hindered by the constraint geometry when the ligand is part of the cage. Second, the dynamics assigned to the P conformer of the open ligand (purple curves) are not observed, because the ligand is trapped in a conformation similar to the AP conformer. Again, a long-lived signal is visible with a lifetime of $\tau_4 = 2.0$ ns (green curves), which was not present for L_O and is therefore attributed to the same dynamics that were already observed for the cycloreversion reaction, namely the deactivation from the ^{3}MLCT state. We can thus conclude that the presence of the two palladium atoms of the supramolecular cage again opens up a competitive deactivation path, i.e. an ISC that forms the ^{3}MLCT state, which reduces the efficiency of the cyclization reaction in the monitored temporal range.

The situation again changes significantly if the three guest molecules are added. The right column of Figure 4 exemplarily shows the transient spectra for the case of five equivalents of the borate dianion (G1@C_{4O}), so that 85 % of the cages are occupied. The PA after 3 ns further decreases (green curves) compared to L_O and C_{4O}, unravelling that the presence of the guest further inhibits the ring-closure reaction. Because the PA is already less pronounced after 30 ps, this is caused by an even less efficient transition through the CI when compared to the empty cage. For the three disparate guests, a similar effect is caused by the guest-

host interaction (see bottom of Figure 4, the green rectangles indicate the reduced yield of ring-closure persisting on long time scales). Hence, we conclude that neither electrostatic interactions nor an enhanced population of the ^{3}MLCT state in case of the ferrocene affect the ultrafast dynamics of the cage. Since the open isomer of the ligand is much more flexible than the closed one, the cage C_{4O} can adapt more easily to the guest than C_{4C} can. Thus, the steric strain induced by the guest molecule may be an explanation as the distortion of the ligand could cause a conformation that has an even lower efficiency for the ring-closure reaction.

Similar to the occupied closed cage, the calculations show that the overall geometry of the open cage does not vary drastically if the disparate guests are added to the cage solution. Table S3 provides selected geometric parameters, e.g. the distance between the two Pd atoms which is only slightly changed when the guests are added to C_{4O}. However, the dihedral angle defined by the two carbon atoms to form the bond upon ring-closure and those of the attached methyl groups (atoms 1, 2, 10, and 11 in Figure S10 and data in Table S3) changes by $\approx 5°$ or more when a guest is introduced, thereby supposably preventing ring-closure to be as effective as without a guest molecule, as also inferable from Table 2. For a complete picture, quantum calculations involving excited-state dynamics would be most appropriate, but the large size of the host–guest systems and the necessity for high-level multireference methods to adequately include conical intersections currently set a too high obstacle.

Conclusion

In summary, there is a strong coherence between the ultrafast cycloreversion and cyclization dynamics of the investigated DTE ligand. The ring-closure and ring-opening both occur with a lifetime of approximately 1 ps and are followed by a vibrational relaxation in the ground state within about 10 ps. However, only the ring-closure reaction is preceded by an ultrafast relaxation in the excited state on a femtosecond timescale. If the ligand is part of the supramolecular Pd^{II}-based cage, a pronounced population of competing reaction pathways is found, i.e. a charge transfer between ligand and Pd atom which is even further increased if the ferrocene guest is inside the closed cage.

With the exception of the ferrocene guest, the ultrafast dynamics of the ligand in the closed cage C_{4C} remain almost unchanged after binding of guest molecules. The situation is very different for the guest-bound open cage $G@C_{4O}$, where the ring-closure of a ligand is significantly reduced for all guests studied here, despite their chemical disparities concerning size, shape, and electrostatic potential. We therefore conclude that steric strain exerted on the cage by the bound guests causes the reduced ring-closure efficiency.

Our studies show that by the encapsulation of a guest molecule in a photoswitchable cage, the guest itself may alter not only the geometry but also the photoinduced dynamics and switching efficiency of the cage. Thus, for applications of controlled guest release by light, the properties of the container and its content should be matched to interfere in a desired fashion. In addition, if an excited cage is intended to interact with an external substrate molecule, e.g. via triplet-triplet energy transfer or a charge-transfer process, inclusion of an appropriate guest molecule might render the reaction more effective due to a suppression of the ultrafast internal conversion in the excited cage, as observed here. Future studies could thus aim at an ideal photocatalytic situation in which a molecule fulfils both functions, being the guest that helps to enhance the desired property of the cage and serving as a substrate.

Acknowledgements

This work was supported by the Research Training Group Confinement-controlled Chemistry, funded by the Deutsche Forschungsgemeinschaft (DFG) under Grant GRK2376/331085229. Open Access funding enabled and organized by Projekt DEAL.

Conflict of Interest

The authors declare no conflict of interest.

Data Availability Statement

The data that support the findings of this study are available from the corresponding author upon reasonable request.

Keywords: Cage Compounds · Confinement · Photoswitches · Supramolecular Chemistry · Ultrafast Spectroscopy

[1] M. Yoshizawa, J. K. Klosterman, M. Fujita, *Angew. Chem. Int. Ed.* **2009**, *48*, 3418–3438; *Angew. Chem.* **2009**, *121*, 3470–3490.
[2] N. Vallavoju, J. Sivaguru, *Chem. Soc. Rev.* **2014**, *43*, 4084–4101.
[3] C. J. Brown, F. D. Toste, R. G. Bergman, K. N. Raymond, *Chem. Rev.* **2015**, *115*, 3012–3035.
[4] S. Saha, I. Regeni, G. H. Clever, *Coord. Chem. Rev.* **2018**, *374*, 1–14.
[5] F. Beuerle, B. Gole, *Angew. Chem. Int. Ed.* **2018**, *57*, 4850–4878; *Angew. Chem.* **2018**, *130*, 4942–4972.
[6] Y. Fang, J. A. Powell, E. Li, Q. Wang, Z. Perry, A. Kirchon, X. Yang, Z. Xiao, C. Zhu, L. Zhang, F. Huang, H.-C. Zhou, *Chem. Soc. Rev.* **2019**, *48*, 4707–4730.
[7] E. G. Percástegui, T. K. Ronson, J. R. Nitschke, *Chem. Rev.* **2020**, *120*, 13480–13544.
[8] A. B. Grommet, M. Feller, R. Klajn, *Nat. Nanotechnol.* **2020**, *15*, 256–271.
[9] M. Morimoto, S. M. Bierschenk, K. T. Xia, R. G. Bergman, K. N. Raymond, F. D. Toste, *Nat. Catal.* **2020**, *3*, 969–984.
[10] B. Huang, L. Mao, X. Shi, H.-B. Yang, *Chem. Sci.* **2021**, *12*, 13648–13663.
[11] Y. Qin, Y.-T. Wang, H.-B. Yang, W. Zhu, *Chem. Synth.* **2021**, *1*, 2.
[12] W. Cullen, H. Takezawa, M. Fujita, *Angew. Chem. Int. Ed.* **2019**, *58*, 9171–9173; *Angew. Chem.* **2019**, *131*, 9269–9271.
[13] A. Das, I. Mandal, R. Venkatramani, J. Dasgupta, *Sci. Adv.* **2019**, *5*, eaav4806.

[14] T. Uchikura, M. Oshima, M. Kawasaki, K. Takahashi, N. Iwasawa, *Angew. Chem. Int. Ed.* **2020**, *59*, 7403–7408; *Angew. Chem.* **2020**, *132*, 7473–7478.
[15] T. N. Lewis, C. Tonnelé, W. G. Shuler, Z. A. Kasun, H. Sato, A. J. Berges, J. R. Rodriguez, M. J. Krische, D. Casanova, C. J. Bardeen, *J. Am. Chem. Soc.* **2021**, *143*, 18548–18558.
[16] A. J. McConnell, C. S. Wood, P. P. Neelakandan, J. R. Nitschke, *Chem. Rev.* **2015**, *115*, 7729–7793.
[17] W. Wang, Y.-X. Wang, H.-B. Yang, *Chem. Soc. Rev.* **2016**, *45*, 2656–2693.
[18] M. Li, L.-J. Chen, Y. Cai, Q. Luo, W. Li, H.-B. Yang, H. Tian, W.-H. Zhu, *Chem* **2019**, *5*, 634–648.
[19] Y. Jiao, Y. Zuo, H. Yang, X. Gao, C. Duan, *Coord. Chem. Rev.* **2021**, *430*, 213648.
[20] H. Lee, J. Tessarolo, D. Langbehn, A. Baksi, R. Herges, G. H. Clever, *J. Am. Chem. Soc.* **2022**, *144*, 3099–3105.
[21] A. D. W. Kennedy, R. G. DiNardi, L. L. Fillbrook, W. A. Donald, J. E. Beves, *Chem. Eur. J.* **2022**, *28*, e202104461.
[22] A. Douhal, T. Fiebig, M. Chachisvilis, A. H. Zewail, *J. Phys. Chem. A* **1998**, *102*, 1657–1660.
[23] D. G. Osborne, J. T. King, J. A. Dunbar, A. M. White, K. J. Kubarych, *J. Chem. Phys.* **2013**, *138*, 144501.
[24] C. J. Otolski, A. Mohan Raj, V. Ramamurthy, C. G. Elles, *J. Phys. Chem. Lett.* **2019**, *10*, 121–127.
[25] N. Alarcos, B. Cohen, M. Ziółek, A. Douhal, *Chem. Rev.* **2017**, *117*, 13639–13720.
[26] J. Nishida, A. Tamimi, H. Fei, S. Pullen, S. Ott, S. M. Cohen, M. D. Fayer, *Proc. Natl. Acad. Sci. USA* **2014**, *111*, 18442–18447.
[27] J. Nishida, M. D. Fayer, *J. Phys. Chem. C* **2017**, *121*, 11880–11890.
[28] Y. Sun, Y. Yao, H. Wang, W. Fu, C. Chen, M. L. Saha, M. Zhang, S. Datta, Z. Zhou, H. Yu, X. Li, P. J. Stang, *J. Am. Chem. Soc.* **2018**, *140*, 12819–12828.
[29] R. Gera, S. L. Meloni, J. M. Anna, *J. Phys. Chem. Lett.* **2019**, *10*, 413–418.
[30] M. Han, R. Michel, B. He, Y.-S. Chen, D. Stalke, M. John, G. H. Clever, *Angew. Chem. Int. Ed.* **2013**, *52*, 1319–1323; *Angew. Chem.* **2013**, *125*, 1358–1362.
[31] M. Han, D. M. Engelhard, G. H. Clever, *Chem. Soc. Rev.* **2014**, *43*, 1848–1860.
[32] R.-J. Li, J. Tessarolo, H. Lee, G. H. Clever, *J. Am. Chem. Soc.* **2021**, *143*, 3865–3873.
[33] R.-J. Li, M. Han, J. Tessarolo, J. J. Holstein, J. Lübben, B. Dittrich, C. Volkmann, M. Finze, C. Jenne, G. H. Clever, *ChemPhotoChem* **2019**, *3*, 378–383.
[34] M. Irie, *Chem. Rev.* **2000**, *100*, 1685–1716.
[35] M. Irie, T. Fukaminato, K. Matsuda, S. Kobatake, *Chem. Rev.* **2014**, *114*, 12174–12277.
[36] M. Herder, B. M. Schmidt, L. Grubert, M. Pätzel, J. Schwarz, S. Hecht, *J. Am. Chem. Soc.* **2015**, *137*, 2738–2747.
[37] M. Kathan, F. Eisenreich, C. Jurissek, A. Dallmann, J. Gurke, S. Hecht, *Nat. Chem.* **2018**, *10*, 1031–1036.
[38] S. Nakamura, M. Irie, *J. Org. Chem.* **1988**, *53*, 6136–6138.
[39] K. Uchida, E. Tsuchida, Y. Aoi, S. Nakamura, M. Irie, *Chem. Lett.* **1999**, *28*, 63–64.
[40] S. Fukumoto, T. Nakashima, T. Kawai, *Angew. Chem. Int. Ed.* **2011**, *50*, 1565–1568; *Angew. Chem.* **2011**, *123*, 1603–1606.
[41] R. T. F. Jukes, V. Adamo, F. Hartl, P. Belser, L. De Cola, *Inorg. Chem.* **2004**, *43*, 2779–2792.
[42] R. T. F. Jukes, V. Adamo, F. Hartl, P. Belser, L. De Cola, *Coord. Chem. Rev.* **2005**, *249*, 1327–1335.
[43] M. T. Indelli, S. Carli, M. Ghirotti, C. Chiorboli, M. Ravaglia, M. Garavelli, F. Scandola, *J. Am. Chem. Soc.* **2008**, *130*, 7286–7299.
[44] I. Hamdi, G. Buntinx, A. Perrier, O. Devos, N. Jaïdane, S. Delbaere, A. K. Tiwari, J. Dubois, M. Takeshita, Y. Wada, S. Aloïse, *Phys. Chem. Chem. Phys.* **2016**, *18*, 28091–28100.
[45] I. Hamdi, G. Buntinx, O. Poizat, S. Delbaere, A. Perrier, R. Yamashita, K. Muraoka, M. Takeshita, S. Aloïse, *Phys. Chem. Chem. Phys.* **2019**, *21*, 6407–6414.
[46] D. Guillaumont, T. Kobayashi, K. Kanda, H. Miyasaka, K. Uchida, S. Kobatake, K. Shibata, S. Nakamura, M. Irie, *J. Phys. Chem. A* **2002**, *106*, 7222–7227.
[47] Y. Asano, A. Murakami, T. Kobayashi, A. Goldberg, D. Guillaumont, S. Yabushita, M. Irie, S. Nakamura, *J. Am. Chem. Soc.* **2004**, *126*, 12112–12120.
[48] T. Sumi, Y. Takagi, A. Yagi, M. Morimoto, M. Irie, *Chem. Commun.* **2014**, *50*, 3928–3930.
[49] M. Irie, T. Eriguchi, T. Takada, K. Uchida, *Tetrahedron* **1997**, *53*, 12263–12271.
[50] J. Ern, A. T. Bens, A. Bock, H.-D. Martin, C. Kryschi, *J. Lumin.* **1998**, *76–77*, 90–94.
[51] J. Ern, A. T. Bens, H.-D. Martin, S. Mukamel, D. Schmid, S. Tretiak, E. Tsiper, C. Kryschi, *Chem. Phys.* **1999**, *246*, 115–125.
[52] J. Ern, A. Bens, H.-D. Martin, S. Mukamel, D. Schmid, S. Tretiak, E. Tsiper, C. Kryschi, *J. Lumin.* **2000**, *87–89*, 742–744.
[53] J. Ern, A. T. Bens, H.-D. Martin, S. Mukamel, S. Tretiak, K. Tsyganenko, K. Kuldova, H. P. Trommsdorff, C. Kryschi, *J. Phys. Chem. A* **2001**, *105*, 1741–1749.
[54] J. Ern, A. T. Bens, H.-D. Martin, K. Kuldova, H. P. Trommsdorff, C. Kryschi, *J. Phys. Chem. A* **2002**, *106*, 1654–1660.
[55] H. Miyasaka, T. Nobuto, M. Murakami, A. Itaya, N. Tamai, M. Irie, *J. Phys. Chem. A* **2002**, *106*, 8096–8102.
[56] Y. Ishibashi, M. Fujiwara, T. Umesato, H. Saito, S. Kobatake, M. Irie, H. Miyasaka, *J. Phys. Chem. C* **2011**, *115*, 4265–4272.
[57] Y. Ishibashi, T. Umesato, S. Kobatake, M. Irie, H. Miyasaka, *J. Phys. Chem. C* **2012**, *116*, 4862–4869.
[58] H. Jean-Ruel, R. R. Cooney, M. Gao, C. Lu, M. A. Kochman, C. A. Morrison, R. J. D. Miller, *J. Phys. Chem. A* **2011**, *115*, 13158–13168.
[59] H. Jean-Ruel, M. Gao, M. A. Kochman, C. Lu, L. C. Liu, R. R. Cooney, C. A. Morrison, R. J. D. Miller, *J. Phys. Chem. B* **2013**, *117*, 15894–15902.
[60] R. J. D. Miller, *Science* **2014**, *343*, 1108–1116.
[61] S. Juber, S. Wingbermühle, P. Nuernberger, G. H. Clever, L. V. Schäfer, *Phys. Chem. Chem. Phys.* **2021**, *23*, 7321–7332.
[62] J. C. Koziar, D. O. Cowan, *Acc. Chem. Res.* **1978**, *11*, 334–341.
[63] S. Lee, Y. You, K. Ohkubo, S. Fukuzumi, W. Nam, *Chem. Sci.* **2014**, *5*, 1463–1474.
[64] M. Frank, J. Ahrens, I. Bejenke, M. Krick, D. Schwarzer, G. H. Clever, *J. Am. Chem. Soc.* **2016**, *138*, 8279–8287.
[65] R.-J. Li, J. J. Holstein, W. G. Hiller, J. Andréasson, G. H. Clever, *J. Am. Chem. Soc.* **2019**, *141*, 2097–2103.
[66] A. Klamt, G. Schüürmann, *J. Chem. Soc. Perkin Trans. 2* **1993**, 799–805.
[67] S. Fredrich, T. Morack, M. Sliwa, S. Hecht, *Chem. Eur. J.* **2020**, *26*, 7672–7677.
[68] P. R. Hania, R. Telesca, L. N. Lucas, A. Pugzlys, J. van Esch, B. L. Feringa, J. G. Snijders, K. Duppen, *J. Phys. Chem. A* **2002**, *106*, 8498–8507.
[69] P. R. Hania, A. Pugzlys, L. N. Lucas, J. J. D. de Jong, B. L. Feringa, J. H. van Esch, H. T. Jonkman, K. Duppen, *J. Phys. Chem. A* **2005**, *109*, 9437–9442.

Manuscript received: August 16, 2022
Accepted manuscript online: September 16, 2022
Version of record online: November 2, 2022